On the heating of ions in the solar corona via non resonant Alfvén wave interaction: neo-adiabatic view of the problem.

Victor Gondret[1, 2, a)]
[1)] *Département de Physique, École Normale Supérieure, Paris, France*
[2)] *Consorzio RFX, CNR, Padova, Italy*

(Dated: 23 August 2018)

The internship report provides a new vision of the heating of ions in the solar corona through Alvén waves. Except the introduction which gives a brief overview of the solar corona problem and some references of the existing literature, the following tries to be more pedagogical with the description of Alvén waves and the complete derivation of the Hamiltonian of a test particle. The neo-adiabatic theory is introduced through the pendulum in a slowly time-modulated gravity field before it is applied to the Alfvénic Hamiltonian. Last part suggests a self-consistent explanation for energy transfer and heating of ions in the solar corona.

I. INTRODUCTION

In 1941, Edlén[1] predicted for the first time a 1 MK temperature in the solar corona through Fe IX and Ca XIV lines. This temperature is much higher than the photospheric temperature which is about 6000 K - or even 4800 K in sunspots. Because of the second law of thermodynamics, heat transfer cannot explain such a difference of temperature, and the puzzle of how the 200 times hotter coronal temperature can be maintained is called the *coronal heating problem*. Many models have been developed to explain this heating. However, they often rely on non-measurable parameters such as magnetic field strength, viscosity, waves, turbulence, etc... It complicates their comparison to experimental data, since most measurements give basic physical parameters, such as density, temperatures, and flow speeds. For the interested reader, a short introduction to some of those models is provided by M. Aschwanden in the chapter 9 of *Physics of the Solar Corona*[2].
In 1942, H. Alvén predicted the existence[3] of "*electromagnetic-hydrodynamic waves*" in a conducting fluid placed in a constant magnetic field and, as soon as 1947, he suggested that those waves might play a role in the coronal heating problem[4]. If the transfer mechanism from waves to particles is still unknown, it has been observed that the energy carried by Alvén waves is sufficient to explain the difference of temperature[5,6], at least in the quiet regions. Indeed, radiative loss scales with density to the power 7/4, thus strong inhomogeneities of the density in the solar corona* imply that heating requirement varies by several orders of magnitude depending on location.

The main obstacle towards the acceptance of Alvén waves as a major coronal heating mechanism was the alleged lack of an effective mechanism of energy transfer from Alvén waves to the ions : under solar conditions, the linear resonance condition between Alvén waves and the cyclotron motion of magnetized ions - the most straightforward and effective mechanism for energy transfer - is hardly fulfilled[7] since the cyclotron frequency in the lower corona may stay in the kHz range (or even more), while most of the spectrum of Alvén waves lies in the mHz range (this value might be increased up to the Hz range according to some authors -see Ryutova 2001 - or when the energy is carried by shock waves - see Zirnstein 2018 - but this does not change qualitatively the problem), and Doppler shift effects are not enough to fill in this gap. In the low-β solar environment a non-self-consistent test-particle approach is reasonable, in which ions are treated as independent particles interacting with a prescribed spectrum of waves. The resulting Hamiltonian system is non-autonomous with a temporal variation parametrized by the ratio between Alvén waves frequency ω and the ion cyclotron one Ω which is extremely slow: $\omega/\Omega \ll 1$. Within this regime, it is intuitive to argue that particle dynamics is adiabatic and that no irreversible transfer of energy from the wave may take place (i.e., no heating)[8,9]. Therefore, the existence of an efficient mechanism for draining energy from the waves to the ions is a non-trivial issue.

Two mechanisms have been proposed in order to overcome this alleged difficulty. First, a series of authors[7,10–13] proposed that the particle trajectories become chaotic† as a consequence of their interaction with a strongly turbulent spectrum of Alvén waves. The decorrelating mechanism is attributed to the coexistence of a set of several waves with different and mutually irrational wavenumbers and frequencies. However, a turbulent wave spectrum is not needed at all: ion motion can be made chaotic even in the presence of a single low-frequency wave. This fact was first noticed experimentally and interpreted by McChesney, Stern, and Bellan [14] in the context of laboratory ion heating by drift-Alfvén waves. White, Chen, and Lin [15], recovering numerically

[a)] Electronic mail: victor.gondret@ens.fr

*The electron density ranges from $n_e \sim 10^6$ cm^{-3} in upper corona to $10^9 - 10^{11}$ cm^{-3} in quiet regions and flare tops.

†Chaotic motion implies irreversible dynamics and hence energy flow.

the same result, provided a unified treatment of longitudinal (electrostatic) and transverse waves, showing how under some constraints the two cases may be mapped into the same formalism. Another paper reaching similar conclusions is Voitenko and Goossens [16]. The numerical parts of these studies converge all to the same qualitative conclusions: a single low-frequency wave can transfer irreversibly energy to ions provided that (i) the amplitude of the wave is large enough, and (ii) the wave propagates obliquely to the ambient magnetic field. Condition (i) stems from the necessity of going beyond the linear approximation; condition (ii) was noticed since long to be necessary for heating to take place[17]. A single Alvén wave propagating parallel to the equilibrium field does not heat ions, but rather transfers reversibly energy, the so-called "pseudo-heating"[12,13]. We will explain extensively in this paper the rationale for this constraint.

White, Chen, and Lin [15] interpret their numerical results in terms of nonlinear resonances: adiabaticity is broken because of the resonance between the wave frequency and the ion guiding-center motion, which takes place at a fraction of the cyclotron frequency, Ω/n. Voitenko and Goossens [16], on the other hand, suggest a different picture. They argue that ions are accelerated non-adiabatically at the occurrence of some matching between the phase of the wave and that of ion motion. Heating, accordingly, does not take place in a continuous fashion but as a sequence of transitions where the adiabatic invariants of the particle change abruptly. Providing an accurate explanation of the breakdown of adiabaticity is a lot more than of academic interest. Indeed, according to the nonlinear resonance picture, when$\omega \to 0$, higher and higher-order resonances need to be excited (since $\omega = \Omega/n$). Intuitively, this requires larger and larger wave amplitudes. This insight looks as supported by numerical results (see Fig. 8 of White, Chen, and Lin [15]), which suggest that heating occurs above a wave amplitude threshold A_m, and that $A_m \to \infty$ as $\omega \to 0$[‡]. As we shall see below, the wave amplitude, written in dimensionless form, is

$$A = (k\rho)(B_\omega/B_0)(u_a/c_s) \tag{1}$$

where k is the wavenumber transverse to the equilibrium magnetic field, ρ the ion thermal Larmor radius, B_ω the amplitude of the magnetic perturbation associated to the wave, B_0 the value of the ambient magnetic field, u_A the Alvén speed, and c_s the ion sound speed. Realistic values for these ratios are $u_a/c_s \sim 10^6/10^5$ (Tomczyk *et. al*[18]) and $B_\omega/B_0 \sim 10^{-1}$ (Esser 1999[19]). As to $k\rho$, the energy spectrum of Alvén waves cascades in the perpendicular wavenumber space, evidencing a stronger damping for , transitioning to kinetic Alvén waves near this threshold[20]; hence looks as a reasonable choice, and is elsewhere employed[16]. Summing it all up, it sounds reasonable to take $A = O(1)$ as the typical wave amplitude.

This work revisits afresh the issue of adiabaticity breaking by Alvén waves, and shows that this breaking simply results from neo-adiabatic theory, developed by several authors three decades ago[21–25] (see the good review of Bazzani [26]). So far, neo-adiabatic theory has been applied within astrophysical contexts to the study of the dynamics of charged particles in the Earth's magnetotail[27,28], but not to the solar corona heating problem, to the best of our knowledge. This theory proves that, in systems whose phase space topology exhibits a separatrix with lobes whose location and area oscillate with time at a frequency ω, the smallness of ω does not imply *per se* adiabatic invariance. Indeed, while adiabatic invariance holds for a particle far from the separatrix, a finite measure of orbits is obliged to cross a pulsating separatrix almost periodically, and each crossing corresponds to the breakdown of adiabatic invariance, since the period diverges on the separatrix. A theorem of neo-adiabatic theory[29,30] proves that the region swept by a pulsating separatrix whose area does not vanish is chaotic. A paradigmatic such system is the pendulum in a slowly time-modulated gravity field[30] that will be studied in the third section of this paper as an introduction to neo-adiabatic theory. Numerically, the time necessary for an orbit to visit the chaotic domain scales as ω^{-3} ; this is backed up analytically by a jump of the adiabatic invariant of order ω at each separatrix crossing and the assumption of the decorrelation of successive jumps occurring over an ω^{-1} time scale[31]. More importantly, neo-adiabatic theory[21–25] shows also that when the area enclosed within the separatrix decreases, trapped and detrapped orbits are divided in different groups, with rotating in opposite directions, which is an abrupt separation of orbits with respect to the familiar exponential one due to chaos. The mathematical analysis presented in this work shows that the system of interest acts similarly, producing a sizeable group of high energy particles after a single separatrix crossing, i.e. over a fast (order ω^{-1}) time scale.

The paper is divided as follows. In section II, properties of Alvén waves and solar corona are recalled. The Hamiltonian of a test particle is derived and simplified. Section III provides the reader Hamiltonian tools used in the following : canonical transformations, action-angle variables, and a proof of the conservation of adiabatic invariant for the harmonic oscillator. Those subsection might be skipped by the informed reader. In the last subsection, the basis of neo-adiabatic theory are introduced through the slowly time dependent pendulum Hamilto-

[‡]The fact that, as $\omega \to 0$, ion heating has to be increasingly difficult to achieve may be argued heuristically since, when ω is rigorously zero, the Hamiltonian system is integrable, hence non-chaotic (This must not be understood as a rigorous reasoning, though, since the static limit is singular).

nian. The discussion of the section and of the all paper will be illustrated by several numerical simulations for which the numerical integration of Hamilton's equations will be performed using the 6^{th}-order symplectic partitioned Runge-Kutta algorithm built into Mathematica software. Section IV introduces the threshold amplitude and deals with the case where the amplitude of the wave A is smaller than 1. In section V, the case $A > 1$ is fully exposed and the change of the adiabatic invariant at each separatrix crossing is explained in an intuitive way. The last subsection introduces a new invariant which is conserved at zero order.

II. ALFVÉN WAVES IN THE SOLAR CORONA

A. Alvén waves and notations

Alvén waves propagate in a magnetized charged fluid. Their existence results from magnetohydrodynamics equations, see *The Physics of Alfvén Waves*[32] for a complete derivation. If one denotes the z axis as the direction of a static axial magnetic field, the dispersion relation for an Alvén wave in a uniform plasma is

$$k_z V_A = \omega, \tag{2}$$

where k_z is the component of the wave vector along z, ω is the pulsation of the wave, and $V_A = B_0/(\mu_0\rho)$ is the Alvén velocity, with B_0 the equilibrium magnetic field and ρ the fluid density. A wave is termed oblique when its direction of propagation is not parallel to the equilibrium magnetic field. In the following, we use the usual $Oxyz$ direct orthonormal frame, and we consider the wave to propagate in the xOz plane, with the wave vector $\vec{k} = k_x\hat{x} + k_z\hat{z}$. It can be shown that, for such an oblique propagation of the wave, the magnetic perturbation is along y and the electric one is along x. Then using Maxwell equations, $\vec{E}$ and $\vec{B}$ fields write

$$\begin{aligned} \vec{E} &= B_\omega V_A \cos(k_x x + k_z z - \omega t)\hat{x}, \\ \vec{B} &= B_0\hat{z} + B_\omega \cos(k_x x + k_z z - \omega t)\hat{y}, \end{aligned} \tag{3}$$

where B_ω is the magnetic amplitude of the wave.
There is a frame where the electric field vanishes and the magnetic fields only depends on position. Such a frame moves toward the equilibrium magnetic field at the Alvén speed, and will be referred as *the Alvén frame*.

B. Derivation of the Hamiltonian

The vector potential in the Alvén frame is

$$\vec{A} = B_0 x\hat{y} + \frac{B_\omega}{k_z}\sin(k_x x + k_z z)\hat{x}.$$

Thus the Hamiltonian of a particle of charge q and mass m in interaction with this field is

$$\begin{aligned} \mathcal{H} = \frac{1}{2m}\left(p_x - qB_\omega k_z^{-1}\sin(k_x x + k_z z)\right)^2 \\ + \frac{1}{2m}\left(p_y - qB_0 x\right) + \frac{p_z^2}{2m}. \end{aligned} \tag{4}$$

Since $\partial\mathcal{H}/\partial y = 0$, p_y is a constant of motion, and one may drop it in the Hamiltonian. The Hamiltonian does not depend on time so it is a constant. Given that $p_x = m\dot{x} + A_x$, the kinetic energy of a particle in the Alvén frame $\frac{1}{2}mv^2$ is conserved. This simplified Hamiltonian leads to two equations of motion:

$$\begin{cases} m\dot{v}_x = -q^2B_0^2(x - x_0)/m - qB_\omega\cos(k_x x + k_z z)v_z \\ m\dot{v}_z = qB_\omega\cos(k_x x + k_z z - \omega t)v_x \end{cases} \tag{5}$$

In the next part, by using some orders of magnitude of our mechanical system in the solar corona, we will simplify this 3D Hamiltonian to obtain a 1D time periodic Hamiltonian.

C. Simplification

The photospheric temperature is about[2] 6000 K. Thus for an ion of typically 10 atomic mass, its velocity is about 3000 $\mathrm{m.s^{-1}}$ whereas it reaches $10 - 100$ $\mathrm{km.s^{-1}}$ in the solar corona. Those velocities should be compared to the Alvén velocity which is about[6] $45 - 200$ $\mathrm{km.s^{-1}}$. First note that photospheric particle velocities are not larger than the corona Alvén velocity. Energy conservation in the Alvén frame implies that, in the laboratory frame, the quantity

$$v_\perp^2 + (V_A - v_\parallel)^2 = \mathrm{Cte}. \tag{6}$$

where $v_\perp$ and $v_\parallel$ are the velocities perpendicular and parallel to the equilibrium magnetic field, is conserved. The particle tends to accelerate along the equilibrium magnetic field and thus its perpendicular velocity must increase. However, since the Alvén velocity is larger than the initial particle one, in the Alvén frame, particle velocity along z can be approximated as $-V_A$. This approximation[§] leads to a unique motion equation that can be written as

$$\frac{k_x}{\Omega_c^2}\frac{\mathrm{d}^2x}{\mathrm{d}t^2} + k_x x = \frac{V_A k_x}{\Omega_c}\frac{B_\omega}{B_0}\cos(k_x x - \omega t), \tag{7}$$

[§]This approximation will no longer be true if the particle is really heated because of the conservation of the energy (Eq. 6). However it leads to an Hamiltonian easier to study and the principle of the study (separation of time scale) remains true. The extension of the results will be discussed in the last section.

where $\Omega_c = qB_0/m$ is the cyclotron frequency. If one expresses time in terms of Ω_c^{-1} and length as k_x^{-1} – which is equivalent to set $\Omega_c = 1$ and $k_x = 1$ – equation (7) reads

$$\ddot{x} + x = A\cos(x - \epsilon t) \quad \text{where} \quad A = \frac{\omega}{\Omega_c}\frac{k_x}{k_z}\frac{B_\omega}{B_0} \tag{8}$$

and $\epsilon = \omega/\Omega_c \ll 1$. The Hamiltonian for this system is therefore

$$\mathcal{H} = \frac{p^2}{2} + \frac{x^2}{2} - A\sin(x - \epsilon t). \tag{9}$$

This Hamiltonian also describes the motion of a charged particle in a uniform magnetic field in interaction with an electrostatic wave propagating across the field[15]. In the next part, we recall familiar concepts of Hamiltonian mechanics : introducing canonical transformations, action-angle variables and the adiabatic invariant. The last part introduces neo-adiabatic theory, which is the basis of our main results. Section IV derives a threshold of chaos for A, the amplitude of the wave in Hamiltonian (4). Section V and VI explain the heating mechanism and why Alvén waves might provide an efficient heating of the solar corona.

III. INTRODUCTION TO NEO-ADIABATIC THEORY

A. Canonical transformations

Let $H(q,p)$ be an Hamiltonian with conjugate variables q and p. A canonical transformation is a change of variable $[Q(q,p,t),\ P(q,p,t)]$ so that the equation of motion are still canonical in the (Q,P) variables. Thus there is a function $\tilde{H}(Q,P,t)$ satisfying

$$\begin{aligned} \frac{\mathrm{d}P}{\mathrm{d}t} &= -\frac{\partial \tilde{H}}{\partial Q} \\ \frac{\mathrm{d}Q}{\mathrm{d}t} &= \frac{\partial \tilde{H}}{\partial P} \end{aligned} \tag{10}$$

and $\tilde{H}$ is the new Hamiltonian in the new conjugate variables. Variational principle ensures the existence of a function F_1 depending for example on q and Q that verifies

$$p\dot{q} - H(q,p,t) = P\dot{Q} - \tilde{H}(Q,P,t) + \frac{\mathrm{d}}{\mathrm{d}t}F_1(q,Q,t). \tag{11}$$

This equation leads to

$$p = \frac{\partial F_1}{\partial q}, \qquad P = -\frac{\partial F_1}{\partial Q}, \qquad \tilde{H} = H + \frac{\partial F_1}{\partial t}. \tag{12}$$

Note that we can also define generating function in terms of other pairs of old and new variables : $F_2(q,P,t)$, $F_3(p,Q,t)$ and $F_4(p,P,t)$. As an example, F_2 can be generate by means of a Legendre transformation $F_2(q,P,t) = F_1(q,Q,t)+QP$ where Q is a function of q and P. Canonical transformation equation can be deduced

$$p = \frac{\partial F_2}{\partial q}, \qquad Q = -\frac{\partial F_2}{\partial J}, \qquad \tilde{H} = H + \frac{\partial F_2}{\partial t}. \tag{13}$$

B. Action-angle variables

Action-angle coordinates (θ, J) are a powerful tool to study integrable Hamiltonian and to apply perturbation theory. We will recall here the basis of this theory for a pendulum Hamiltonian but the interested reader could refer to Lichtenberg and Lieberman [33] for the general case. For a general one-degree-of-freedom, the action is defined as

$$J \mathrel{\widehat{=}} \frac{1}{2\pi}\oint p\,\mathrm{d}q. \tag{14}$$

For a pendulum Hamiltonian, $H = p^2/2 - \omega_0^2\cos(q)$, the action can be geometrically defined as the area within the orbit for trapped libration. For untrapped rotation, the action is defined as the area between the orbit and the q-axis for $q \in [-\pi, \pi]$ as shown in Fig. 1. With this definition, J is a constant of the motion and the Hamiltonian (energy) is a function of J only $H = H(J)$. The value of J defines full orbit[¶]. To complete the set of new coordinates, one has to introduce the angle θ, conjugate coordinate of the action, defined as

$$\theta = \frac{\partial \phi}{\partial J} \quad \text{where} \quad \phi(J,q) = \int_{q_0}^{q} p(I,q')\mathrm{d}q' \tag{15}$$

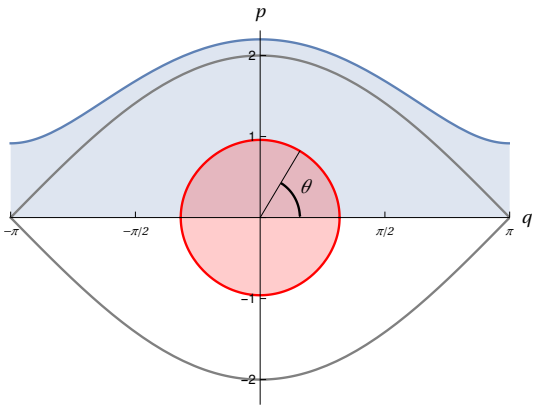

FIG. 1: Sketch of areas used in the definition of action. The adiabatic invariant is the area in blue for unbounded rotating trajectories and in red for bounded librating ones. The grey line represent the separatrix which separates bounded and unbounded trajectories.

Since the Hamiltonian is a function of J only, Hamilton's equations lead to $\dot{J} = 0$ (the action is conserved) and to

$$\dot{\theta} = \frac{\partial \mathcal{H}_0}{\partial J} \mathrel{\widehat{=}} \Omega(J),$$

[¶] As we shall see in the following, it is convenient to define the action for bounded motion with a factor 1/2 so that the action is continuous at the separatrix.

which means that the period of an orbit with action I is $2\pi/\Omega(J)$. Note that the time needed to reach the X point is infinite, therefore the frequency on the separatrix is zero $\Omega(J) = 0$.
We now display the action-angle transformation for the harmonic oscillator (which corresponds to low-energies trajectories for the pendulum) $H' = p^2/(2m) + \omega_0^2 q^2/2 = E_0$

$$J = \frac{2}{\pi}\int_0^{q_{max}} \sqrt{2E_0 - \omega_0^2 q^2}\,\mathrm{d}q = \frac{E_0}{\omega_0}.$$

and J is again an invariant of motion. The Hamiltonian in the new coordinate writes $\tilde{\mathcal{H}}_0' = \omega_0 J$. To define the coordinate conjugate to the action, we use the type 2 generating function

$$F = \int_0^q \sqrt{2\omega_0 J - \omega_0^2 q^2}\ \mathrm{d}q.$$

Thus, θ is defined as

$$\theta = \frac{\partial F}{\partial J} = \omega_0 \int_0^q \left(2\omega_0 J - \omega_0^2 q^2\right)^{-1/2}\ \mathrm{d}q, \tag{16}$$

and p and q can be deduced by using

$$q = (2J/\omega_0)^{1/2}\sin\theta, \qquad p = (2J\omega_0)^{1/2}\cos\theta. \tag{17}$$

This transformation is usually performed by using the type 1 generating function $F_1 = \frac{1}{2}\omega_0 q^2\cot\theta$. This transformation can be really useful to develop the Hamiltonian as a series in some small parameter.

C. Adiabatic invariant

We saw in the previous section that J is a constant of motion, as the energy when the Hamiltonian does not depend on time. However, when for example ω_0 is a slowly function of time, to lowest order in the slowness parameter J does not vary from its initial value even if ω_0 and $\tilde{\mathcal{H}}_0'$ change by large amount : J is said to be the lowest order *adiabatic invariant*. Here again we will show this for an harmonic oscillator - which corresponds to small energies for a pendulum - for didactic purpose. For the Hamiltonian $\tilde{\mathcal{H}}_0'$, the characteristic frequency is ω_0 thus the Hamiltonian varies slowly with time if

$$\frac{1}{\omega_0}\frac{\mathrm{d}\omega_0}{\mathrm{d}t} \ll \omega_0.$$

In this case, J is an adiabatic invariant. Let's show this for a slowly harmonic oscillator[33] $\mathcal{H} = p^2/2 + \omega^2(\tau)q^2/2$ where the mass m is set to one and $\tau = \epsilon t$. Using the generating function $F_1 = \frac{1}{2}\omega_0 q^2\cot\theta$ and Eq. (12), the transformed Hamiltonian writes as

$$\tilde{\mathcal{H}} = \omega J + \epsilon\frac{1}{2}\frac{\omega'}{\omega}J\sin 2\theta, \tag{18}$$

where $'$ denotes differentiation with respect to τ. To zero order, the adiabatic invariant is just H_0/ω_0 and is constant. Let now consider the new type 1 transformation - close to identity - from (θ, J) to $(\theta_\epsilon, J_\epsilon)$

$$\begin{aligned} F_1^*(\theta, J_\epsilon) &= \theta J_\epsilon + \epsilon\frac{\omega'}{4\omega}J_\epsilon\cos 2\theta \\ &\sim \theta J_\epsilon + \epsilon\frac{\omega'}{4\omega}J\cos 2\theta \end{aligned} \tag{19}$$

where we replaced J_ϵ by J for a first order approximation. Then, one gets

$$J_\epsilon = \omega J(1 + \epsilon\frac{1}{2}\frac{\omega'}{\omega^2}\sin 2\theta) \tag{20}$$

If one takes the time derivative of J_ϵ, two terms of the right hand-side of 20 will vanish thanks to Hamilton's equation. Thus, up to first order in ϵ

$$\dot{J}_\epsilon = \epsilon\frac{J}{2}\sin\theta\,\frac{\mathrm{d}(\omega'/\omega^2)}{\mathrm{d}t}.$$

However,

$$\frac{\mathrm{d}}{\mathrm{d}t}(\frac{\omega'}{\omega^2}) \sim \epsilon\frac{\omega'}{\omega^2}$$

which means that the action is constant to first order in ϵ, (indeed $\dot{J}_\epsilon \sim \epsilon^2$).
In the following of this section, we will consider the slowly time-dependent Hamiltonian

$$\begin{aligned} H &= p^2/2 - \omega_0^2(\epsilon t)\cos(q) \\ &\text{with} \quad \omega_0^2(\epsilon t) = 1 + A\cos(\epsilon t). \end{aligned} \tag{21}$$

The previous result shows that the action is conserved for trajectories with an energy lower than ω_0^2 and it can be shown[33] that the action is also conserved for trajectories with energies greater than ω_0^2. To check this conservation, we integrated motion equation and reported at each period $2\pi/\epsilon$ of the amplitude the position of the particle in the phase space. Such a plot is called a stroboscopic plot (we observe the system periodically), and is a special instance of the famous Poincarré map. If the action is conserved, we should observe that the different points sketch an orbit with a constant energy trajectory. Figure 2, realized with $\epsilon = 0.05$ and $A = 1/2$ shows indeed that the action - the energy - is conserved away from the yellow area. The dashed gray curves correspond to the position of the separatrix at $t = 0$ and $t = \pi/\epsilon$, which pulsates within the thin layer indicated by the yellow area.

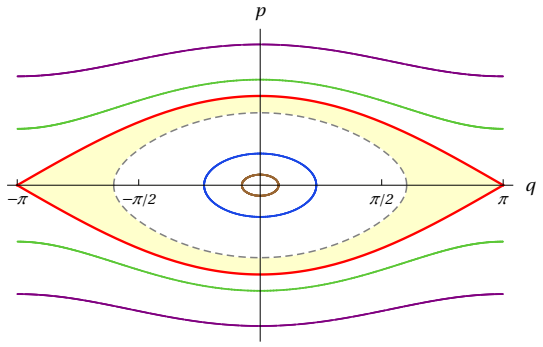

FIG. 2: Stroboscopic plot in the phase space for 4 different trajectories (purple, green, blue and brown) with parameters $\epsilon = 0.05$ and $A = 1/2$. The red curve represents the separatrix at time $t = 2\pi n\epsilon^{-1}$, $n \in \mathbb{N}$ and the yellow area is the chaotic area.

As we will show in the next part, the adiabatic invariant and the energy is no longer conserved for orbits for which the action is between two critical values. Upper value is given by the maximal area between the separatrix and the q-axis, the lower one by the minimal area. The area between these two extrema is the chaotic area. It takes different shapes depending on the time of the stroboscopic plot.

D. Destruction of the adiabatic invariant: the neo-adiabatic theory

Adiabatic theory relies on the existence of two different time scales, one fast - the movement of the particle - and one slow - the motion of the separatrix. However, near the separatrix, the period of trajectories diverges and thus the assumption of adiabatic theory is no longer true. When a particle is close to the separatrix and crosses it, its adiabatic invariant and energy are slightly changed.

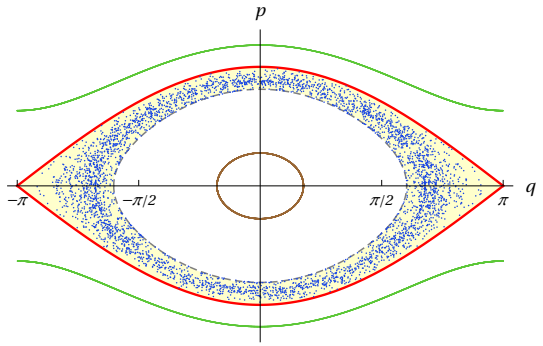

FIG. 3: Stroboscopic plot in the phase space for 3 different trajectories with parameters $\epsilon = 0.05$ and $A = 1/2$. The initial energy of the green orbit is greater than $1+A$, the one of the brown orbit is smaller than $1-A$ and the initial energy of the blue is between those two *critical* energies.

If one considers a particle with an adiabatic invariant between between $\int_{-\pi}^{\pi}\sqrt{(1-A)(1+\cos q)}\mathrm{d}q$ - half[‖] of the minimal area enclosed by the separatrix - and $\int_{-\pi}^{\pi}\sqrt{(1+A)(1+\cos q)}\mathrm{d}q$ - half of the maximal area - the particle will have to cross the separatrix twice at each period. When the instantaneous period of the particle become greater than the separatrix period, adiabatic invariance is destroyed. The adiabatic invariant experiences a little jump which can be computed. The value of this jump[21] is of order ϵ and depends on the phase of the particle - its position - at the crossing.

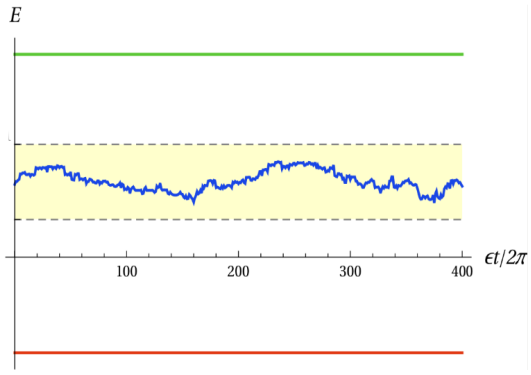

FIG. 4: Energy of 3 orbits at each period of the wave. Blue curve is the chaotic orbit (same orbit than the blue of Fig. 3), red curve a bounded orbit (same orbit than the brown of Fig. 3) and green curve an unbounded one (same orbit than the green of Fig. 3). Those energies match with the stroboscopic plot of Fig. 3. Dashed gray lines represent the critical energies beyond which orbits are regular.

Fig. 4 shows that, if the energy of particles out of the "pulsated" area are well-conserved as expected, it is not the case for the blue particle whose energy looks has having a random walk and if one takes an ensemble of particles with a given energy and an uniform distribution in phase, the evolution of the distribution in energy will be a gaussian of width $\sigma(\epsilon t)$.
Fig. 5 displays a gaussian fit to the energy histogram at different times. The width of the gaussian, still at first order in ϵ, grows as the square root of the time with a diffusion coefficient proportional to[21] ϵ^3. This means that the typical time for chaos to develop is proportional to ϵ^{-3} and thus it can be very hard (painful numerical integration of motion) to observe it numerically for very low frequencies.

[‖] Half of the area because we had a 1/2 factor in the definition of the adiabatic moment for rotations

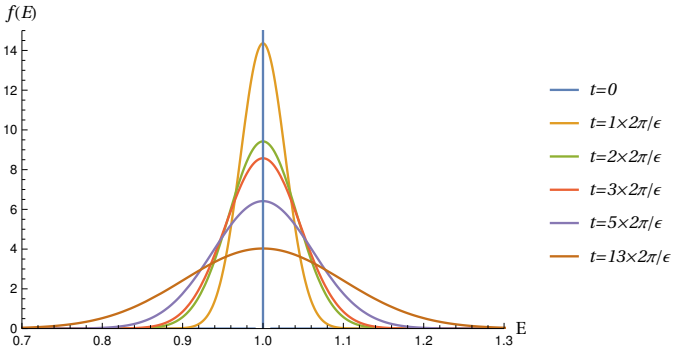

FIG. 5: Evolution of the energy distribution (normalized) starting with a delta distribution in energy ($E_0 = 1$), uniform in phase with 3000 particles.

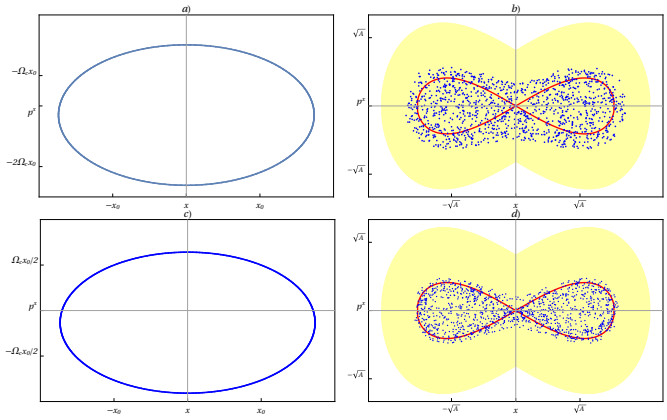

FIG. 6: Stroboscopic plots ($\epsilon t \equiv \pi$) of the phase space for $\epsilon = 10^{-2}$ with $A = 0.8$ (a) and $A = 1.3$ (b) and for $\epsilon = 10^{-3}$ and $A = 0.8$ (c) and $A = 1.3$ (d). In yellow, the area swept by the separatrix and in red the separatrix at $\epsilon t = \pi$. The initial condition for the particle used are $x_0 = 0,03$ and $p_{x,0}) = 0$.

IV. PRELIMINARY RESULTS AND LOW AMPLITUDE WAVES

In this section, we come back to the one dimensional Hamiltonian derived in section II. We will see some general results from numerical simulation and will treat the case of low amplitude waves and derive a threshold that depends on the frequency of the wave. We recall that the Hamiltonian is

$$\mathcal{H} = \frac{p^2}{2} + V(x,\lambda), \quad \text{with } V(x,\lambda) = \frac{x^2}{2} - A\cos(x-\lambda), \tag{22}$$

where $\lambda = \epsilon t$ varies slowly with time.

A. Preliminary results

When the amplitude A of the Hamiltonian of Eq. 22 is greater than 1, the potential V might have a local maximum - for some time - and thus a separatrix might exist in the phase space. Neo-adiabatic theory exposed in the previous section with the pendulum example predicts that orbits with an adiabatic invariant between the maximal and the minimal area surrounded by the separatrix are chaotic. Here, the separatrix has two lobes one initially big that decreases to a point and the other one initially a point grows. The chaotic area concerns therefore orbits with adiabatic invariant between 0 and the maximum area surrounded by the separatrix which will be called he maximal invariant. Since the chaotic area contains the origin of the phase space, one can expect law energy particle to spread in the phase space and therefore increase the total energy and speak of *heating*. When $A < 1$, there is no separatrix in the phase space therefore neo-adiabatic theory cannot explain heating. The stroboscopic plots of the phase space of Fig. 6 shows that chaos occurs for both frequency $\epsilon = 10^{-2}$ and $\epsilon = 10^{-3}$ when $A > 1$, whereas the trajectory of particles are not chaotic when $A < 1$ for those same frequency.

This figure and the fact that chaos occurs when a separatrix exists shows that neo-adiabatic theory is a good way to explain the development of chaos for this system. However, as remarked by White, Chen, and Lin [15] and by numerical simulations, one can observ that chaos does develop even when $A < 1$ but close to 1. The two next subsection will be dedicated to the case $A < 1$ while the next section will focus on the $A > 1$ case.

B. Linearisation for low amplitudes

When $A < 1$, potential $V(x,\lambda)$ has a single minimum at all time λ and this minimum can be labelled by $x_m(t)$ (see Fig. 7). This minimum verifies - or is even defined by

$$\frac{\partial V}{\partial x}\,|_{x_m} = x_m + A\sin(x_m - \lambda) = 0. \tag{23}$$

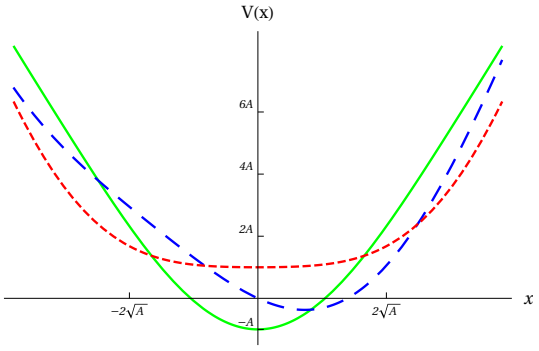

FIG. 7: Potential for $A = 0,9$ at different time $\lambda = 0$ (green), $\lambda = \pi/2$ (blue, dashed) and $\lambda = \pi$ (red, dots).

A particle starting with low energy will follow this minimum. It is therefore natural to decompose the position of

the particle as $x = x_m + \delta x$ where x_m varies slowly with time and δx is the fast variable. When $A = 0$, $x_m = 0$ and the movement of δx is the one of the usual harmonic oscillator. In this case, a good approach of the problem is of course to treat the wave as a perturbation[34]. However, this study does not provide any proof of heating when frequency is much lower (more than "only" ten times) than cyclotron frequency. Deriving equations of motion from Eq. 22 and using Eq. 23, to first older in δx, motion equation reads

$$\begin{aligned} \ddot{\delta x} + \Omega^2 \delta x &= -\ddot{x}_M + \mathcal{O}(\delta x^2) \\ \text{where } \Omega(\epsilon t) &= \sqrt{1 + A\cos(x_M - \epsilon t)}. \end{aligned} \tag{24}$$

Given the definition of x_M, it is obvious that x_M and thus $\ddot{x}_M$ are $2\pi/\omega$-periodic functions and can be decomposed as a Fourier series $x_m(t) = \sum_n C_n \sin(n\epsilon t)$. Eq. (24) is therefore the equation for an harmonic oscillator of frequency Ω (which vary with time) forced by a $2\pi/\omega$-periodic function. The standard resonant condition for an harmonic oscillator is that excitation frequency should be equal to the system frequency. By superposition, the problem can be reduced to

$$\ddot{\delta x}^{(n)} + \Omega^2 \delta x^{(n)} = \beta_n \sin(n\epsilon t). \tag{25}$$

where $\beta_n = C_n n^2 \epsilon^2$ and $\delta x = \sum_n \delta x^{(n)}$.

The minimum of Ω is $\sqrt{1-A}$, reached when $\epsilon t \sim \pi$, therefore when $\sqrt{1-A} \sim n\epsilon$, there is a resonance. Since the resonance condition is valid for a finite time only, the final energy of the particle will depend on its initial conditions - how the particle will be in phase with the excitation. Two nearby orbits might diverge from each other which is the signature of chaos. The condition

$$A \sim 1 - \epsilon^2 \tag{26}$$

is therefore a sufficient condition to have heating.

C. Neo-adiabatic view of the problem

We saw that, when the instantaneous period of an orbit is greater than the period of the wave, adiabatic invariance is broken and it chaos develops. Since $\dot{x} = \partial H/\partial p$, instantaneous period is given by

$$T = \oint \frac{\mathrm{d}x}{\partial H/\partial p} = \oint \frac{\mathrm{d}x}{\sqrt{2h - x^2 - 2A\cos(x-\lambda)}}, \tag{27}$$

where the integral follows the trajectory of a particle of energy h at $\lambda = \epsilon t$ fixed. If this period is greater or of same order of the period of the wave, adiabatic theory assumption ($T \ll \epsilon^{-1}$) is no longer true and one expects adiabatic invariant not to be conserved. Instantaneous period of a trajectory is directly related to the spacing between the two branches of the potential. It is clear, using the Fig. 7, that the maximal period is expected to be around $\lambda = \pi$. For very low energy particles, one can expand the cosinus in potential V and the energy of a particle can be approximated by $h = A + (1-A)X^2/2 + \mathcal{O}(X^4)$ where X is the maximal position of the trajectory. Instantaneous period is therefore given by

$$T \sim \int_{-X}^{X} \frac{\mathrm{d}x}{\sqrt{(1-A)X^2/2 - (1-A)x^2/2}} \sim \frac{2\sqrt{h-A}}{1-A}. \tag{28}$$

The inequality $X < 1$ (to guarantee that the expansion for the cosinus was true), implies that $h < 1$. In fact, the energy is also greater than A. Taking a particle of energy $(1+A)/2$ leads to a break of the adiabatic invariant when

$$T \sim \frac{1}{\sqrt{1-A}} \sim \epsilon^{-1}, \tag{29}$$

which is the same conclusion than the previous result.
To conclude, we saw that it exists a threshold amplitude $A_c \sim 1 - \epsilon^2$ below which chaos occurs. This threshold limit goes to one when $\epsilon \to 0$ however, behaviour of orbits changes dramatically when amplitude is greater than 1. This case will be study in the following section.

V. WAVE AMPLITUDE GREATER THAN 1

When $A > 1$, the potential may have a local maximum depending on the value of A and time. Cary, Escande, and Tennyson [21] calculated the change of the adiabatic invariant at each separarix crossing at different order in ϵ. In the previous example with the pendulum, at each separatrix crossing, the adiabatic invariant was continuous at the crossing and the change was of order ϵ, depending on the phase of the orbit. Here, the change of lobe is not continuous, even at zeroth order: when an orbit crosses the separatrix, the adiabatic invariant is changed by a *large* amount.
The first subsection will be dedicated to the study of separatrix and lobes. The next subsection will treat of orbit transfer while the last one will focus on the introduction of a conserved quantity - function of the adiabatic invariant - which will be called the *Alfvénic invariant*.

A. Motion of separatrix and lobes

When $A > 1$, the potential may have a local maximum depending on the value of A and time. The potential can even have several maxima however, we will restrict to the case $A \in [1, 4.5]$ which means that there is either 0 or 1 minimum depending on time. We define by $\tilde{\lambda}$ the time at which the local maximum appears. Given the symmetry of the potential with time, the maximum disappears at $\lambda = 2\pi - \tilde{\lambda}$. When there is a maximum, a separatrix (red) exists in the phase space splitting the whole domain in three different areas: two lobes labelled a (left lobe) and b (right lobe) and the area outside those lobes labelled c. They are represented for different time

in Fig. 8.

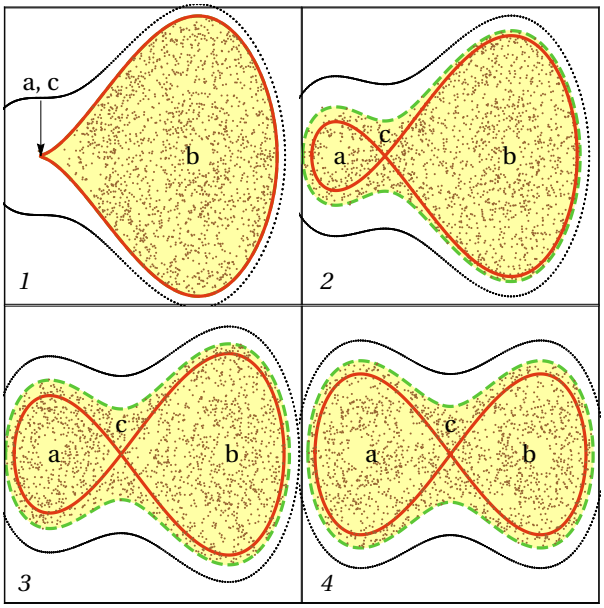

FIG. 8: Separatrix (red solid curve) in the (x,p) phase space at time $\tilde{\lambda}$ (1, the separatrix has just appeared), two times at regular interval between $\tilde{\lambda}$ and π (2 and 3) and at time $\lambda = \pi$ (4, the two lobes are identical: we are at half the period of the wave). The second half-period evolves with mirror symmetry. The yellow area is the chaotic area, defined as the area enclosed by the trajectory (green dotted) of an orbit of the frozen system with an adiabatic invariant equal to the critical adiabatic invariant $\tilde{\mathcal{J}}$. Black dots and brown dots are the stroboscopic plots for a regular and a chaotic orbit numerically integrated with w = 0,01. The figure has been produced with A = 3 but is totally generic.

Fig. 8.1 represents the separatrix (red) at time $\tilde{\lambda}$. Lobe a and region c are reduced to a point. So far, we did not define the upper limit for region c : from now we will define it as the orbit of the frozen system (λ fixed) for which the adiabatic invariant is equal to the area enclosed by the separatrix at time $\tilde{\lambda}$. This area is will refer to the critical adiabatic invariant and will be noted $\tilde{\mathcal{J}}$. Critical orbit with adiabatic invariant $\tilde{\mathcal{J}}$ (green dashed line) and separatrix (red) are represented on Fig. 8 at time $\lambda = \tilde{\lambda}$ (1)**, two times between $\tilde{\lambda}$ and π (2 and 3) and at time $\lambda = \pi$ (4). Stroboscopic plot of two orbits is also provide for an orbit with adiabatic invariant greater than $\tilde{\mathcal{J}}$ (black dots) and smaller (brown dots). The black dots are aligned on a curve, showing that the motion is regular : the adiabatic invariant of the orbit is greater than the critical adiabatic invariant therefore the adiabatic invariant of the orbit is conserved. On the opposite, orbits with adiabatic invariant smaller than $\tilde{\mathcal{J}}$ are chaotic which is well illustrated by the sea of brown dots on Fig. 8.

When a lobe decreases, a given set of orbits must escape and cross the separatrix. In fact, the flux of orbits that leaves a lobe is given by the time derivative of the area of the lobe. This flux is kept by other areas accordingly to their respective growth rate. This is why the time evolution of lobes are very important to explain how chaos develops. The evolution of each lobe is shown in Fig. 9 for $A = 3$.

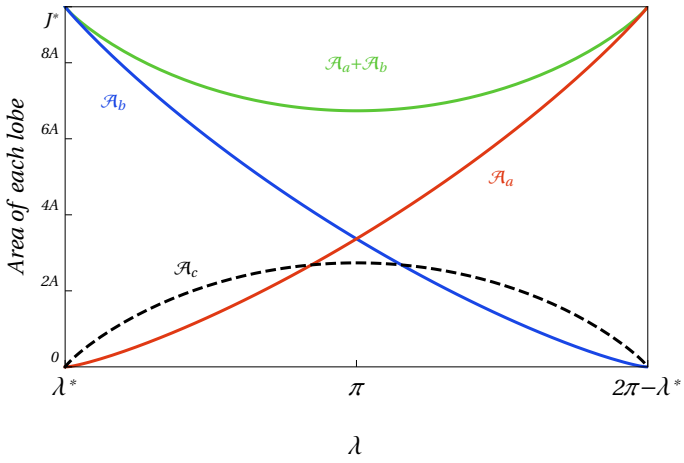

FIG. 9: Area of lobe a (red curve, labelled $\mathscr{A}_a$), lobe b (blue curve, labelled $\mathscr{A}_b$) and region c (black dashed curve, labelled $\mathscr{A}_c$). Green curve on top represents the sum of areas of lobe a and b. The figure has been produced with $A = 3$ but is totally generic.

The function $\lambda \mapsto \mathscr{A}_b$ is a bijection so that it is possible to express each quantity plotted here as a function of $\mathscr{A}_b$ *e.g.* each time the lobe b has a given area $\mathscr{A}_b$, the lobe a has an area $\mathscr{A}_a(\mathscr{A}_b)$, the time at which the area of lobe b is $\mathscr{A}_b$ is $\lambda(\mathscr{A}_b)$ and the region c has an area $\mathscr{A}_c(\mathscr{A}_b)$. It is therefore natural to define a mapping between $\mathscr{A}_a$ and $\mathscr{A}_b$, so we define the function

$$\begin{array}{rccc} \mathcal{F} & : & [0,\tilde{\mathcal{J}}] & \to & [0,\tilde{\mathcal{J}}] \\ & & \mathscr{A} & \mapsto & \mathcal{F}(\mathscr{A}) \end{array} \tag{30}$$

When the lobe b has an area $\mathscr{A}_b$, the lobe a has an area $\mathscr{A}_a = \mathcal{F}(\mathscr{A}_b)$. Reciprocally, since the potential evolves with mirror symmetry with respect to π, when the lobe a has an area $\mathscr{A}_a$, the lobe b has an area $\mathscr{A}_b = \mathcal{F}(\mathscr{A}_a)$. This symmetry implies a nice property for $\mathcal{F}$ which is

$$\mathcal{F} \circ \mathcal{F} = \mathrm{Id}. \tag{31}$$

An other property of $\mathcal{F}$ is that it does not depend on time. To any area between $[0,\tilde{\mathcal{J}}]$ it is possible to map an other area within the same interval *no matter the time, no matter the existence or not of a separatrix in*

**At $\lambda = \tilde{\lambda}$, separatrix and critical orbit are overlaid.

the phase space. The notion of lobe area has of course a sense only between $\tilde{\lambda}$ and $2\pi - \tilde{\lambda}$ however, once $\mathcal{F}$ is defined, its definition does not rely any more on time. This non-dependence of $\mathcal{F}$ with time or presence of a separatrix is fundamental for the following. Finally, $\mathcal{F}$ has a fixed point that will be noted $J_\pi = \mathcal{F}(J_\pi)$. Note that this fixed point corresponds to the area of lobe b and a at time π.

As it has been shown in section III, the adiabatic invariant corresponds to the area enclosed by the orbit in the frozen system. The adiabatic invariant for a chaotic orbit is within the interval $[0, \tilde{\mathcal{J}}]$ so that one can associate a conjugated invariant $\mathcal{F}(J)$ at any orbit within the chaotic area with an adiabatic invariant J. This function is the blue solid curve on Fig. 10 while the green dashed curve is the function $J \mapsto \mathcal{F}(J) + J$.

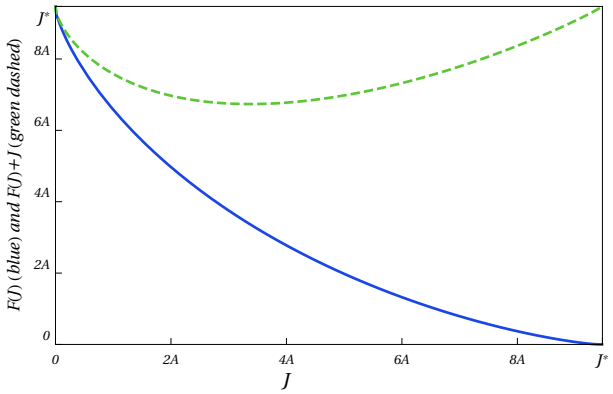

FIG. 10: The blue solid curve represents the variation of $\mathcal{F}$ with J while the green dashed curve is the function $\mathcal{F}(J) + J$.

Finally, a last function Λ can be introduced.

$$\begin{array}{ccccc} \Lambda & : & [0, \tilde{\mathcal{J}}] & \to & [\tilde{\lambda}, 2\pi - \tilde{\lambda}] \\ & & J & \mapsto & \Lambda(J) \end{array} \tag{32}$$

This function maps a given adiabatic invariant J to the time $\Lambda(J)$ at which lobe b has the same area as J *e.g.* the time at which $\mathscr{A}_b(\Lambda(J)) = J$. For the same symmetry reason seen previously, Λ verifies $\Lambda \circ \mathcal{F}(J) = 2\pi - \Lambda(J)$. Now that we defined those functions and we studied the evolution of lobes, we will see how orbits of this Hamiltonian evolve.

B. Transfer of orbits

In this part, we will explain the separatrix crossing of orbits with initial small adiabatic invariant *e.g.* smaller than J_π and we will neglect the adiabatic invariant change of order ϵ to focus on the change of order A. Consider an orbit of adiabatic invariant J_1 at time $\lambda = 0$. We will suppose that $J_1 < J_\pi$ and will see the case $J_1 > J_\pi$ latter. At time $\lambda = 0$, there is no separatrix, it appears only at time $\tilde{\lambda}$. The orbit changes of lobe when the area of lobe b matches to its adiabatic invariant J_1 therefore crossing happens at time $\Lambda(J_1)$. Since we suppose that $J_1 < J_\pi$, crossing time $\Lambda(J_1)$ is smaller that π. Between $[\pi, 2\pi - \tilde{\lambda}]$, areas b and c decrease therefore orbits exiting one of those area can only enter lobe a[††]. At zeroth order, right before the crossing time, at $\lambda = \Lambda(J_1)^-$, the orbit fits with lobe b separatrix while at time $\lambda = \Lambda(J_1)^+$, after the lobe change, orbit hugs the lobe a separatrix. Fig. 11 shows the transfer of an orbit from lobe b to lobe a.

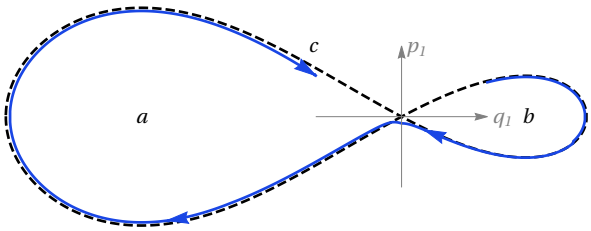

FIG. 11: Jump of an orbit (blue) with initial adiabatic invariant $J_1 < J_\pi$ from lobe b to lobe a. Black dashed curve represent the separatrix. Separatrix crossing happens at $\lambda = \Lambda(J_1) > \pi$.

Fig. 11 and previous reasoning can deduce the new adiabatic invariant of the orbit: since particle trajectory as time $\Lambda(J_1)^+$ hugs lobe a separatrix, its new adiabatic invariant J_2 is equal to the area of lobe a which means $J_2 = \mathcal{F}(J_1)$. Once the crossing happened, new orbit's adiabatic invariant is conserved (adiabatic theory applies) therefore it and is still $J_2 = \mathcal{F}(J_1)$ at time $\lambda = 2\pi$. The following is straightforward : the quantity

$$\mathcal{I} = J + \mathcal{F}(J). \tag{33}$$

is conserved[‡‡]. In the next subsection, we will show that this quantity is indeed conserved for a transfer $J > J_\pi$.

C. Defining a new invariant

We will now consider an orbit with initial adiabatic invariant $J_2 > J_\pi$ at time $\lambda = 0$. $J_2 = \mathcal{F}(J_1)$ and we will show that its Alfvénic invariant is conserved. For this case, $\Lambda(J_2) < \pi$ therefore when the orbit has to jump from lobe b to an other area, it has two possibilities: either it enters lobe a, either area c.[§§]

[††] This is not totally true, to enter lobe a, orbits from lobe b must pass through c. However, the typical time they stay in area c is short : it is a double-crossing.

[‡‡] At time $\lambda < \Lambda(J_1)$, $\mathcal{I}_1 = J_1 + \mathcal{F}(J_1)$ while at time $\lambda > \Lambda(J_1)$, this quantity is $\mathcal{I}_2 = J_2 + \mathcal{F}(J_2)$ however since $\mathcal{F}(J_1) = J_2$ and $\mathcal{F}^2 = \mathrm{Id}$, we have $\mathcal{I}_1 = \mathcal{I}_2$. □

[§§] We recall that the number of orbits entering area c rather than lobe a is proportional to the ratio of the growing rate of each area.

Consider first the orbit does a single crossing and stay in area c (see Fig. 12). Here again, we consider that the orbits fits the separatrix therefore, in the area c, its new adiabatic invariant is the sum of the two lobe area which corresponds to $J_2 + \mathcal{F}(J_2)$. To have a continuity of the Alfvénic invariant at a single separatrix crossing $b \to c$, the Alfvénic invariant must be define as

$$\mathcal{I} \mathrel{\widehat{=}} J = \oint p\mathrm{d}x \quad \text{in area } c. \tag{34}$$

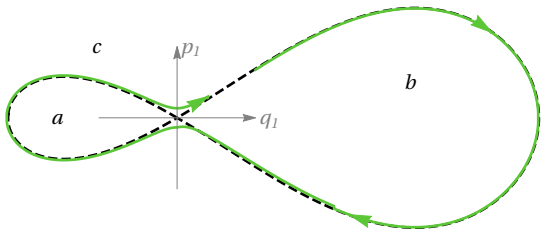

FIG. 12: Single crossing of an orbit (green) of initial adiabatic invariant $J_2 > J_\pi$ from lobe b to area c. Black dashed curve represent the separatrix. Separatrix crossing happens at $\lambda = \Lambda(J_2) < \pi$

After $\lambda = \pi$, area of region c decreases until it reaches 0 at $2\pi - \tilde{\lambda}$ therefore orbits will have to enter lobe a before separatrix disappears. Again, the orbit will enter lobe a when its adiabatic invariant $J_2 + \mathcal{F}(J_2)$ will be equal to the sum of lobe a and b. Crossing happens at time $2\pi - \Lambda(J_2) = \Lambda \circ \mathcal{F}(J_2)$ and the new adiabatic invariant of the orbit is the size of lobe a in which orbit enters (see Fig. 13). At this time, lobe a area is equal to J_2 therefore new adiabatic invariant of the orbit is J_2 and its Alfvénic invariant is $\mathcal{I} = J_2 + \mathcal{J}_2$ (definition in lobe a) and $\mathcal{I}$ is continuous at the separatrix crossing. Since its adiabatic invariant will be constant until time $\lambda = 2\pi$, the Alfvénic invariant is constant over a period.
To summarize, we just showed that, when an orbit with initial adiabatic invariant $J_2 > J_\pi$ enters area c, its Alfvénic invariant (defined in lobe b by Eq. 34) is constant the whole period.

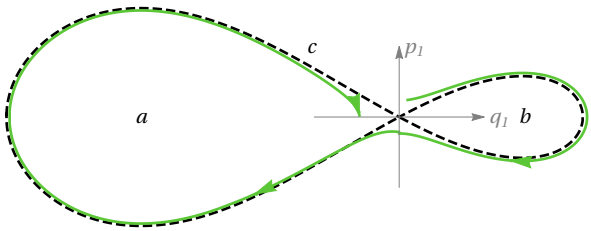

FIG. 13: An orbit (green) in area c with adiabatic invariant $J_2 + \mathcal{F}(J_2)$ entering lobe a. Black dashed curve represent the separatrix. Separatrix crossing happens at $\lambda = \Lambda \circ \mathcal{F}(J_2) > \pi$

Now we suppose the orbit of adiabatic invariant $J_2 > J_\pi$ makes a double crossing and enter directly lobe a at time $\Lambda(J_2)$. At $\lambda = \Lambda(J_2)$, lobe a area is $\mathcal{F}(J_2)$ therefore the new adiabatic invariant J_3 of the orbit is $J_3 = \mathcal{F}(J_2)$ and new Alfvénic invariant of the orbit is $\mathcal{I}_3 = J_3 + \mathcal{F}(J_3) = \mathcal{F}(J_2) + \mathcal{F} \circ \mathcal{F}(J_2) = \mathcal{I}_2$. After the crossing, lobe a keeps growing thus the orbit is away from the separatrix and its adiabatic invariant and Alfvénic invariant are constant. Here again, we showed the Alfvénic invariant is conserved when the orbits enters directly lobe a.

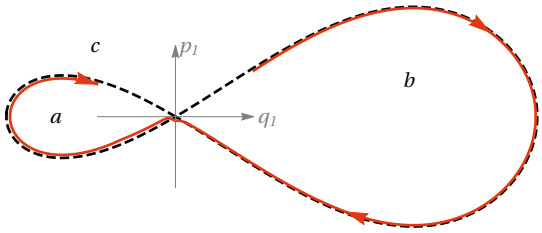

FIG. 14: Double crossing of an orbit (green) of initial adiabatic invariant $J_2 > J_\pi$ from lobe b to lobe a. Black dashed curve represent the separatrix. Separatrix crossing happens at $\lambda = \Lambda(J_2) < \pi$

To conclude, in this subsection, we introduced a new quantity, function of the adiabatic invariant, which is conserved at separatrix crossing. This quantity, the Alfvénic invariant, is defined as

$$\mathcal{I} \mathrel{\widehat{=}} \begin{cases} J + \mathcal{F}(J) & \text{in lobe a, lobe b and when there is no separatrix.} \\ J & \text{in lobe c} \end{cases} . \tag{35}$$

For the pendulum like Hamiltonian treated in section III, we saw that during a separatrix crossing, adiabatic invariance is destroyed because the time scale separation on which relies adiabatic theory is no longer true. Here, we saw that the adiabatic invariant is even not conserved at order zero in ϵ this is why we constructed the Alfvénic invariant. However, as it was the case for the pendulum-like Hamiltonian, the Alfvénic invariant will no longer be conserved.

VI. STATISTICS ON ORBITS TRANSFER AND HEATING OF THE SOLAR CORONA

In section III, we saw that the typical time for chaos to develop scaled, for the pendulum, as the frequency to the power -3. If we assume the same scaling for the diffusion of the Alfvénic invariant in our system, typical scale time for chaos to develop is about $10^{15}\Omega_c^{-1}$. This value is too big to consider the heating realistic. We will see in this section how Alfvénic invariant conservation rather than adiabatic invariant conservation changes radically the time scale for heating.

A. Statistics on orbit transfer

We will interest here in the energy at times $\lambda = 2n\pi$ with $n \in \mathbb{N}$ so that there is a bijection between adiabatic moment and energy. Indeed, the quantity that does interest physicist is particles energy since measurements give speed of particles. We will index each quantity by n to refer at what time the quantity is measured and we will suppose that n is small enough so that Alfvénic invariant is conserved. This assumption is equivalent to neglect the change of order ϵ in the adiabatic invariant when an orbit crosses the separatrix and seems reasonable since $\epsilon \sim 10^{-5}$. Initially, we start with cold ions $E_0 \sim -A$ and $J_0 \sim 0$ and we want to know if the average energy per particle did increase or not after n period. To do so, some properties must be recalled.

1. When a particle has an adiabatic invariant $J < J_\pi$, its adiabatic invariant after one period is $\mathcal{F}(J) > J_\pi$.

2. When a particle has an adiabatic invariant $J > J_\pi$, its adiabatic invariant after one period is either $\mathcal{F}(J) < J_\pi$ either $J > J_\pi$, depending on the phase of the orbit. The probability that its adiabatic invariant is conserved after one period depends only on J and is noted μ_J.

The first property is just a trivial consequence of section V B : since $\Lambda(J) > \pi$, particle must enter lobe a which has an area greater than J_π.
The second is deduced by the fact that the number of orbits entering area c rather than lobe a is proportional to the ratio of the growing rate of each area. Crossing happens at time $\lambda = \Lambda(J) < \pi$ therefore, by noting $\mathscr{A}_a$ (resp. $\mathscr{A}_c$) the area of lobe a (resp. lobe c), the probability μ_J for an orbit to go in lobe c verifies

$$\frac{\mu_J}{1-\mu_J} = \left.\frac{\mathscr{A}_c'}{\mathscr{A}_a'}\right|_{\Lambda(J)} \qquad \text{where } \mathscr{A}_i' \,\widehat{=}\, \frac{\mathrm{d}\mathscr{A}_i}{\mathrm{d}\lambda} \tag{36}$$

In fact, since $\mu_j = \mu_{\mathcal{F}(J)}$, the probability μ_J depends even only on the Alfvénic invariant. If we start with $\mathcal{N}$ particles with same adiabatic invariant, they split into two groups at each period. One group with low energy[¶¶] E_- and adiabatic invariant J_- and an other group with high energy E_+ and adiabatic invariant $J_+ = \mathcal{F}(J_-) > J_\pi$. The number of particle with energy E_- (resp. E_+) at time $\lambda = 2n\pi$ is noted $\mathcal{N}_n^-$ (resp. $\mathcal{N}_n^+$) and the evolution of an ensemble of particle verifies

$$\begin{cases} \mathcal{N}_{n+1}^+ = \mathcal{N}_n^- + \mu_J \mathcal{N}_n^+ \\ \mathcal{N}_{n+1}^- = (1-\mu_J)\mathcal{N}_n^+ \end{cases} \tag{37}$$

for which the unique possible limit is

$$\mathcal{N}^+ = \frac{\mathcal{N}}{2-\mu_J} \qquad , \qquad \mathcal{N}^- = \mathcal{N}\frac{1-\mu_j}{2-\mu_J} \tag{38}$$

B. Heating of ions in solar corona conditions

On the Fig. 10, the growing rate of $\mathscr{A}_a$ at $\lambda = \tilde{\lambda}$ is null therefore $\mu_J(J=0) = \mu_J(J=\tilde{\mathcal{J}}) = 1$ when an orbits has an invariant equals to the maximal adiabatic invariant $\tilde{\mathcal{J}}$, the orbit cannot come back to lobe a and have an adiabatic invariant equal to zero. The same thing happens when $\lambda = \pi$: the growing rate of $\mathscr{A}_c$ is zero and $\mu_J(J = J_\pi) = 0$: the orbit must enter lobe a.
More generally, if the initial adiabatic invariant of an orbit is close to 0, it is more likely that the orbit will have a high adiabatic invariant: μ is a decreasing function of J on $[0, J_\pi]$ and an increasing function on $[J_\pi, \tilde{\mathcal{J}}]$. This can be summarize by the following sentence: given an ensemble of particle with same energy, the lower the initial energy is, the higher the final average energy will be.

It is also important to underline that the heating[***] happens on a very short time scale: only one period is enough! This is very important because Alvén waves appear and disappear and their life duration should be lower than the time needed for chaos to fully develop - which is proportional to ω^{-3}. After a few period of interaction, the energy gain by a particle is of order A. This scaling with ω^{-1} rather than ω^{-3} is also important to justify the test-particle approach: the collision frequency ranges in the mHz like the frequency of the wave therefore they must be taken into account when one deals with time scale of order ω^{-3}.

C. Numerical simulation

To illustrate the last subsections, it is possible to consider an ensemble of 2000 ions with same initial energy of order $-A$ therefore initial adiabatic invariant almost null. They only differ by their phase, which is distributed uniformly. This simulation was performed with $A = 3$ and $\omega = 0.01$. At each period of the wave ($t = 0$, ν^{-1}, $2\nu^{-1}$, $8\nu^{-1}$, $16\nu^{-1}$ and $50\nu^{-1}$), the histogram of the adiabatic invariant is represented in Fig. 15. We start initially a Dirac distribution ($t = 0$) for ions in adiabatic invariant centred at J_0. After one period,the distribution is centred on $\mathcal{F}(J_0)$ as expected but we already see the spread of the distribution function due to the adiabatic invariant change of order ϵ. After two periods, the two peaks of the distribution function are visible

[¶¶] An energy is said low when the adiabatic invariant corresponding to this energy is lower than J_π.

[***] By heating we mean increase of the average energy

and for longer time, the spread of each peak increases. Here, the spread of each peaks is quite clear because the frequency is 0.01, however, when ω is of order 10^{-5}, 10^{-6}, we can expect the spreading to be lower after the same number of period.

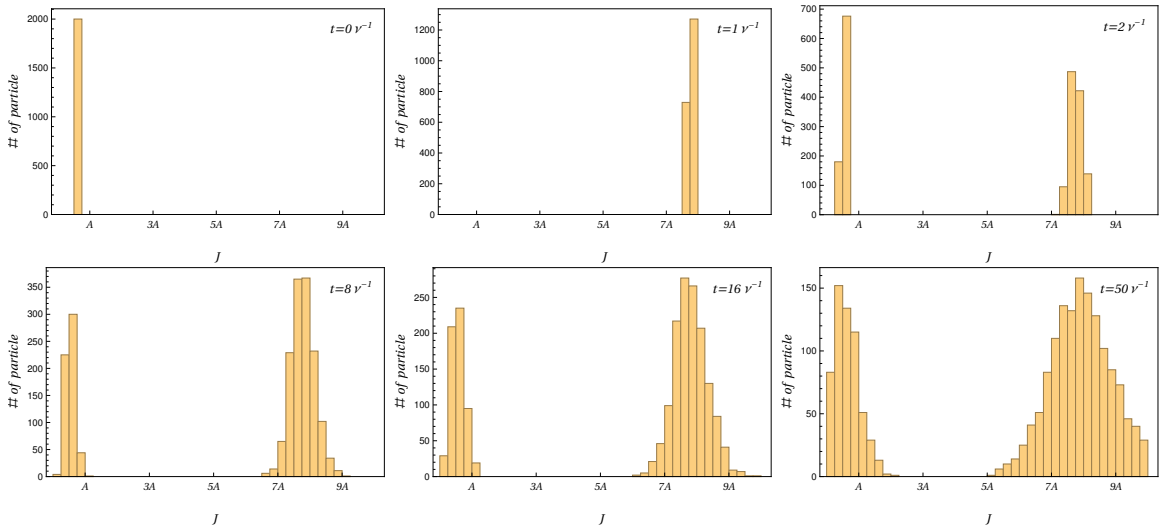

FIG. 15: Distribution function of the adiabatic invariant starting with ions with initial adiabatic invariant of $0.7A$ interacting with a wave with parameters $A = 3$ and $\omega = 0.01$. The distribution function is shown at $t = 0$ and after 1, 2, 8, 16 and 50 periods.

VII. CONCLUSION

We showed that, for wave amplitudes $A > 1$, starting with low kinetic energy particles, we get after a few period a non-negligible fraction of them with a energy that increased by a value of order A. However, the ion could gain energy when the wave is present and lost it when the wave disappears. A particle initially at rest gains eventually some speed and kinetic energy, for any finite value of A. This is the ion pick-up mechanism by the wave well known in literature[35,36]. By itself, this is not a proper heating since the energy flow is reversible and is returned fully to the wave once the interaction is switched off. In order to make it irreversible, it must be supplemented by some dissipative mechanism, such as collisions or the chaos due to the pulsating separatrix. Fig.16 makes visual the net effect due to this latter mechanism. In this case, the waveform has been modulated by a shape function

$$A(t) = A\left(1+\tanh(\frac{t-t_i}{\tau})\right)\left(1+\tanh(\frac{t_f-t}{\tau})\right) \quad (39)$$

such that there is no wave for $t < t_i$ and $t > t_f$. It may be regarded as a rough modeling of the interaction between an initially cold ion and a burst of magnetic activity, e.g, a flare. In the Fig. 16, we plot the instantaneous energy $\mathcal{H}(t)$ from Eq. (22) for several different choices of A. For values below unity no energy is left to the particle after the wave vanishes; conversely, there is a net increase in energy for those cases where $A > 1$. When $A < 1$, ion gain energy when the wave is present and the notion of "pseudo-heating" introduced by Wang and Wu [12] makes sense: ion velocity increases when the wave is present while it decreases when the wave is turned off adiabatically.

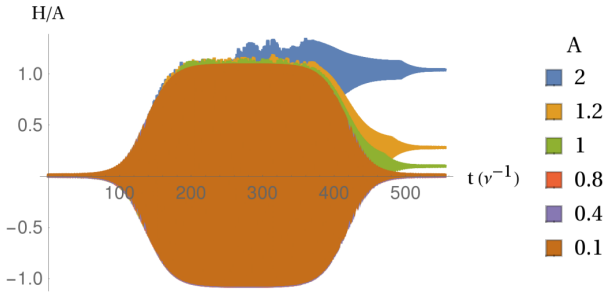

FIG. 16: Energy of an ion as a function of time. The different curve represent different amplitudes. Parameters for the shape function are $\tau = 100\nu^{-1}$, $t_i = 130\nu^{-1}$ and $t_f = 430\nu^{-1}$.

During the derivation of the one-dimensional Hamiltonian, we neglected the z velocity compare to the Alvén velocity. However, by using the kinetic energy conservation in the Alvén frame, it is possible to show that when particle are heated, their velocity among x increases enough to accelerate the particle among z and the approximation might be false. Neishtadt and Vasiliev [37] proved that neo-adiabatic theory applies also

to two dimensional system where it exists a fast variable ($k_x x$ in our system) and a slow variable ($k_z z$). The reasoning developed before applies by replacing ωt by $\omega t - k_z z$.

To summarize, we have just shown that a particle initially at rest, after having interacted with an Alfvén wave for a duration as short as a single wave cycle, may gain a finite amount of energy $E_f = O(A) = O(1)$ e.g. ions reach energies of the order of the coronal temperature: when A is about 2, $E_f = k_B T$ where k_B is the Boltzmann constant, and T is the coronal ion temperature. This result prompts us to the following speculation: for the actual flows of ions and Alfvén waves into the corona, its temperature is the one corresponding to the full conversion of the Alfvén wave power into the thermal power injected into the solar wind. Together with this scenario, a self-organization process occurs: if A is below 1, the transfer of energy from Alfvén waves to ions is weak, and there is a pile up of Alfvén wave energy, which increases A above 1. Then the transfer of energy to ions described above sets in and increases with A. The pile-up of Alfvén waves can be justified on the basis that there is no smooth transition from the corona to the solar wind. This occurs through the so-called "coronal holes" corresponding to (rare) zones where the magnetic field lines are open and where the plasma is less dense and colder. Less reconnection is likely to occur in such zones, and thus less generation of Alfvén waves. In contrast the hot corona corresponds to magnetic loops where Alfvén waves are trapped and can pile up.

VIII. ACKNOWLEDGEMENT

This report is the result of my internship in Consorzio RFX, Padova. For this internship, I was daily supervised by Fabio Sattin. I would like to express my sincere gratitude to him for his warm welcome, kindness, and dedication. This project was initiated by Dominique Escande, whom I also want to thank for their assistance, teaching, and the valuable interactions we had.

[1] B. Edlén, "An attempt to identify the emission lines in the spectrum of the solar corona," Arkiv for Matematik Astronomi och Fysik **28B** (1941), 10.1093/mnras/107.2.211.

[2] M. Aschwanden, *Physics of the Solar Corona* (Springer, 2005).

[3] H. Alfvén, "Existence of electromagnetic-hydrodynamic waves," Nature **150**, 406 (1942).

[4] H. Alfvén, "Magneto hydrodynamic waves, and the heating of the solar corona," Royal Astronomical Society **107**, 211–219 (1947).

[5] D. B. Jess, M. Mathioudakis, R. Erdélyi, P. J. Crockett, F. P. Keenan, and D. J. Christian, "Alfvén waves in the lower solar atmosphere," Science **323**, 1582–1585 (2009).

[6] B. De Pontieu, S. W. McIntosh, M. Carlsson, V. H. Hansteen, T. D. Tarbell, C. J. Schrijver, A. M. Title, R. A. Shine, S. Tsuneta, Y. Katsukawa, K. Ichimoto, Y. Suematsu, T. Shimizu, and S. Nagata, "Chromospheric alfvénic waves strong enough to power the solar wind," Science **318**, 1574–1577 (2007).

[7] C. B. Wang, C. S. Wu, and P. H. Yoon, "Heating of ions by alfvén waves via nonresonant interactions," Phys. Rev. Lett. **96**, 125001 (2006).

[8] R. M. Kulsrud, "Adiabatic invariant of the harmonic oscillator," Phys. Rev. **106**, 205–207 (1957).

[9] A. Lenard, "Adiabatic invariance to all orders," Annals of Physics **6**, 261 – 276 (1959).

[10] J. Heyvaerts and E. Priest, "Coronal heating by phase-mixed shear alfvén waves," Astronomy and Astrophysics **117**, 220–234 (1983).

[11] O. Y. Kolesnychenko, V. V. Lutsenko, and R. B. White, "Ion acceleration in plasmas with alfvén waves," Physics of Plasmas **12**, 102101 (2005), https://doi.org/10.1063/1.2052133.

[12] C. B. Wang and C. S. Wu, "Pseudoheating of protons in the presence of alfvénic turbulence," Physics of Plasmas **16**, 020703 (2009), https://doi.org/10.1063/1.3068472.

[13] C. Dong and N. Singh, "Ion pseudoheating by low-frequency alfvén waves revisited," Physics of Plasmas **20**, 012121 (2013), https://doi.org/10.1063/1.4789608.

[14] J. M. McChesney, R. A. Stern, and P. M. Bellan, "Observation of fast stochastic ion heating by drift waves," Phys. Rev. Lett. **59**, 1436–1439 (1987).

[15] R. White, L. Chen, and Z. Lin, "Resonant plasma heating below the cyclotron frequency," Physics of Plasmas **9**, 1890–1897 (2002), https://doi.org/10.1063/1.1445180.

[16] Y. Voitenko and M. Goossens, "Cross-field heating of coronal ions by low-frequency kinetic alfvén waves," The Astrophysical Journal Letters **605**, L149 (2004).

[17] Y. Lin and L. C. Lee, "Structure of reconnection layers in the magnetosphere," Space Science Reviews **65**, 59–179 (1993).

[18] S. Tomczyk, S. W. McIntosh, S. L. Keil, P. G. Judge, T. Schad, D. H. Seeley, and J. Edmondson, "Alfvén waves in the solar corona," Science **317**, 1192–1196 (2007), http://science.sciencemag.org/content/317/5842/1192.full.pdf.

[19] R. Esser, S. Fineschi, D. Dobrzycka, S. R. Habbal, R. J. Edgar, J. C. Raymond, J. L. Kohl, and M. Guhathakurta, "Plasma properties in coronal holes derived from measurements of minor ion spectral lines and polarized white light intensity," The Astrophysical Journal Letters **510**, L63 (1999).

[20] S. D. Bale, P. J. Kellogg, F. S. Mozer, T. S. Horbury, and H. Reme, "Measurement of the electric fluctuation spectrum of magnetohydrodynamic turbulence," Phys. Rev. Lett. **94**, 215002 (2005).

[21] J. R. Cary, D. F. Escande, and J. L. Tennyson, "Adiabatic-invariant change due to separatrix crossing," *Physical Review A*, **34**, 4256–4275 (1986).

[22] J. L. Tennyson, J. R. Cary, and D. F. Escande, "Change of the adiabatic invariant due to separatrix crossing," Phys. Rev. Lett. **56**, 2117–2120 (1986).

[23] J. H. Hannay, "Accuracy loss of action invariance in adiabatic change of a one-freedom hamiltonian," Journal of Physics A: Mathematical and General **19**, L1067 (1986).

[24] A. Neishtadt, "Variation of adiabatic invariant crossing the separatrix, fiz," (1986).

[25] A. N. Vasil'ev and M. A. Guzev, "Particle capture by a slowly varying periodic potential," Theoretical and Mathematical Physics **68**, 907–916 (1986).

[26] A. Bazzani, "Adiabatic invariance for pendulum-like systems," Il Nuovo Cimento A (1971-1996) **112**, 437–446 (1999).

[27] J. Chen, "Nonlinear dynamics of charged particles in the magnetotail," Journal of Geophysical Research: Space Physics **97**, 15011–15050 (1992).

[28] A. Ukhorskiy, M. Sitnov, R. Millan, and B. Kress, "The role of drift orbit bifurcations in energization and loss of electrons in the outer radiation belt," Journal of Geophysical Research: Space Physics **116** (2011).

[29] Y. Elskens and D. F. Escande, "Slowly pulsating separatrices sweep homoclinic tangles where islands must be small: an extension of classical adiabatic theory," Nonlinearity **4**, 615–667 (1991).

[30]Y. Elskens and D. Escande, "Infinite resonance overlap: a natural limit for hamiltonian chaos," Physica D: Nonlinear Phenomena **62**, 66 – 74 (1993).
[31]D. L. Bruhwiler and J. R. Cary, "Diffusion of trajectories in a simple hamiltonian system with slow periodic forcing," Computer Physics Communications **65**, 52 – 56 (1991).
[32]N. Cramer, *The Physics of Alfven Waves* (Wiley, 2011).
[33]Lichtenberg and Lieberman, *Regular and Stochastic Motion* (Springer New York, 1983).
[34]C.-R. Choi, M.-H. Woo, K. Dokgo, K.-W. Min, D.-Y. Lee, P. H. Yoon, J. Hwang, J.-J. Lee, and Y.-D. Park, "Ion temperature anisotropy due to perpendicular heating by alfvén wave propagating along magnetic field lines," Physics of Plasmas **23**, 092903 (2016), https://doi.org/10.1063/1.4963389.
[35]X. Li, Q. Lu, and B. Li, "Ion pickup by finite amplitude parallel propagating alfvén waves," The Astrophysical Journal Letters **661**, L105 (2007).
[36]E. J. Zirnstein, D. J. McComas, R. Kumar, H. A. Elliott, J. R. Szalay, C. B. Olkin, J. Spencer, S. A. Stern, and L. A. Young, "In situ observations of preferential pickup ion heating at an interplanetary shock," Phys. Rev. Lett. **121**, 075102 (2018).
[37]A. I. Neishtadt and A. A. Vasiliev, "Destruction of adiabatic invariance at resonances in slow fast Hamiltonian systems," Nuclear Instruments and Methods in Physics Research A **561**, 158–165 (2006), nlin/0511050.